Apparent phonon side band modes in π-conjugated systems: polymers, oligomers and crystals

E. Ehrenfreund[1], C.C. Wu[2], Z.V. Vardeny[2]
[1] *Department of Physics, Technion–Israel Institute of Technology, Haifa 32000, Israel*
[2] *Department of Physics, University of Utah, Salt Lake City, UT 84112*

The emission spectra of many π-conjugated polymers and oligomers contain side-band replicas with apparent frequencies that do not match the Raman active mode frequencies. Using a time dependent model we show that in such many mode systems, the increased damping of the time dependent transition dipole moment correlation function results in an effective elimination of the vibrational modes from the emission spectrum; subsequently causing the appearance of a regularly spaced progression at a new apparent frequency. We use this damping dependent vibrational reshaping to quantitatively account for the vibronic structure in the emission spectra of π-conjugated systems in the form of films, dilute solutions and single crystals. In particular, we show that by using the experimentally measured Raman spectrum we can account in detail for the apparent progression frequencies and their relative intensities in the emission spectrum.

Keywords: Optical absorption and emission spectroscopy, Photoluminescence, Raman spectroscopy, Conjugated and/or conducting polymers

1. Introduction

The typical photoluminescence (PL) spectrum of many π-conjugated systems is composed of vibronic progression series (e.g., Fig. 1a, [1]). One key feature of the vibronic progression is that it contains side-band replicas with apparent frequencies that do not match the measured Raman active modes (e.g., Fig. 1b, [1]). In many cases the rich Raman spectrum is reduced to only one or two vibronic progression in the emission spectrum, not necessarily having the same frequencies as the most intense Raman modes. In this work we account for the apparent modes that appear in the PL spectra of π-conjugated systems, such as polymers, oligomers and single crystals. We use the measured pre-resonance Raman spectra in order to quantify the relative configuration displacement (or, equivalently, the Huang-Rhys factor) for each of the modes. We then utilize these relative Huang-Rhys (HR) factors in a damped time dependent model for the PL emission. We show that the apparent vibronic frequencies in the PL spectrum are the result of a "weighted beating" of all Raman frequencies. These frequencies are not, in general, the simple average of the Raman frequencies, and thus cannot be predicted a priori. Furthermore, the relative intensities of the apparent vibronic structure are uniquely determined by their strengths in the Raman spectrum.

2. Time dependent multi-vibrational analysis of photoluminescence

In order to account for the PL spectrum of a multi-vibrational system in relation to its Raman spectrum, it is useful to employ time dependent analysis rather than the often used sum-over-states Franck-Condon approach [2]. We write the PL spectrum, F(E), as a Fourier transform [3]:

$$F(E) = \int_{-\infty}^{\infty} f(t)\exp\left(\frac{iEt}{\hbar}\right) dt \ . \tag{1}$$

where the dipole correlation function, f(t), is given by:

$$f(t) = |P|^2 \exp\left[\frac{-iE_0 t}{\hbar} - S + S_+(t) + S_-(t) - \Gamma|t|\right] \ . \tag{2}$$

In Eq. (2), P is the dipole matrix element and E_0 is the bare energy for the relevant optical transition. S and $S_\pm(t)$ are given by the following sums over the vibration modes:

$$\begin{aligned} S_+(t) &= \sum_j S_j(n_j+1)\exp(-i\omega_j t) \ ; \\ S_-(t) &= \sum_j S_j n_j \exp(i\omega_j t) \ ; \\ S &= \sum_j S_j(2n_j+1) \ , \end{aligned} \tag{3}$$

where ω_j are the Raman mode frequencies, n_j are the equilibrium mode populations according to the Bose-Einstein distribution, $S_j = \omega_j \Delta_j^2 / 2\hbar$ (Δ_j is the mode equilibrium displacement in the optically excited electronic state relative to the ground state) are identified as the mode HR factors, whereas S=S(T) is the total temperature dependent HR factor. We emphasize here that it is the "electron temperature", T_e, which determines the mode occupation, n_j. T_e is determined by the photon excitation energy and the electron excess energy relaxation rate and may be considerably higher than the lattice temperature, T. The time dependent term $S_+(t)$ is responsible for the red shifted vibronic side bands in the PL spectrum, while the $S_-(t)$ term gives rise to blue

shifted (due to a "hot luminescence" process) side bands, which may appear for low frequency modes at relatively high temperatures. In Eq. (2) we introduced a simple mode independent phenomenological damping parameter Γ; it represents losses due to natural line broadening and/or other degrees of freedom [4].

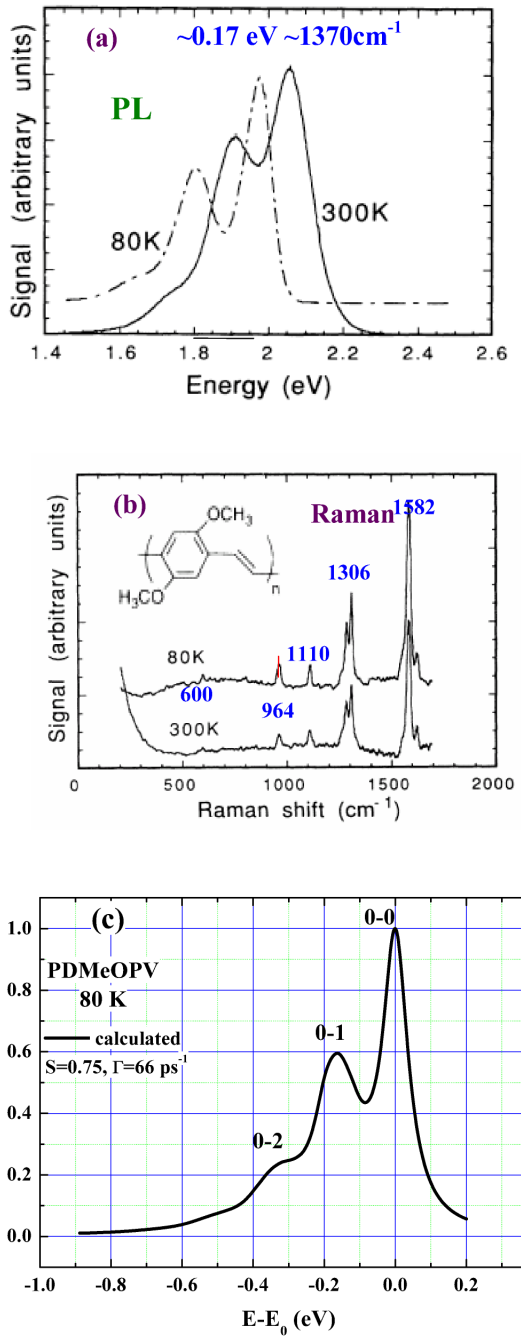

FIG. 1. (a) PL spectrum of PDMeOPV; showing a single vibronic frequency at ≈1370 cm^{-1}. (b) Raman spectrum of PDMeOPV. The Raman frequencies are marked. Inset: chemical structure. (Data from: Woo et. al., Ref. [1]). (c) Calculated PL spectrum using the data of Fig. 1b and Eqs. 1-3. The resulting vibronic separation is ≈1350 cm^{-1}. Energy is measured relative to the 0-0 transition energy (E_0).

The HR factors that determine the vibronic structure are closely related to the measured Raman spectrum, since the Raman process is enabled by the same electron-phonon interaction. The T=0 K intensity, I_j^0, of each Raman line measures its excited state displacement Δ_j [2]: $I_j^0 \propto \omega_j^2$; we then have: $S_j \propto I_j^0/\omega_j^2$. We note the proportionality of S_j to ω_j^{-2}, which emphasizes the contribution of lower frequency Raman modes to the vibronic structure in the PL emission.

As an example for the above analysis, we consider films of poly(dimethoxy phenylene vinylene) [PDMeOPV]. Using the Raman data published previously [1] (Fig. 1b), we have calculated the expected PL vibronic structure. This is shown in Fig. 1c. As seen, the calculated spectrum is in agreement with the experimental spectrum: (a) Both spectra are composed of a single vibronic progression; (b) The calculated progression frequency of ≈ 0.16 eV in the PL spectrum (Fig. 1c) is very close to the measured one (Fig. 1a). A choice of total HR factor of S(0)=0.75 and damping of Γ=66 ps^{-1} yields relative intensities and line broadening similar to that measured at T=80 K.

3. The case of distyryl-benzene

The excited state properties of distyryl-benzene (DSB), which is the three phenyl group oligomer of p-phenylene vinylene (Fig. 2a, inset), have been the subject of recent experimental [5,6] and theoretical [7] spectroscopic studies, because of potential opto-electronic applications [8]. DSB PL spectroscopy has been the subject of numerous research studies, since it is strongly dependent upon the packing order. The first excited state of isolated DSB molecules is optically allowed, making them strongly luminescent and useable as active media in light emitting devices [8]. The room temperature PL spectrum of isolated DSB molecules consists of the fundamental ("0-0") optical transition and a single apparent frequency phonon side band replica series. In DSB films the molecules form H aggregates, thus substantially weakening the PL emission quantum yield relative to the isolated oligomers in dilute solutions [9]. This is especially true in DSB single crystals: due to the herring bone symmetry the fundamental optical transition is either totally absent or significantly reduced [9]. Typical PL spectra of DSB chromophores contain vibronic progression series, of which the relative intensity and frequencies depend on the packing and temperature. The PL emission spectra of crystalline DSB are discussed elsewhere [10]. Here, we discuss only our results for dilute solutions, which reflect the single molecule PL spectrum.

3.1. DSB solution

In Table I we list the most intense Raman modes observed for DSB. The Raman spectra for the solution or crystalline forms are similar. Here we present the crystalline data since its signal to noise ratio is much better.

Along with the frequencies and relative intensities, we list for each mode the deduced relative HR factor, calculated using the model discussed in Section 2 and the Raman data presented in Fig. 2. It is important to recognize that the lowest frequency mode has the largest HR factor, although its intensity is only ≈1% of the strongest line!

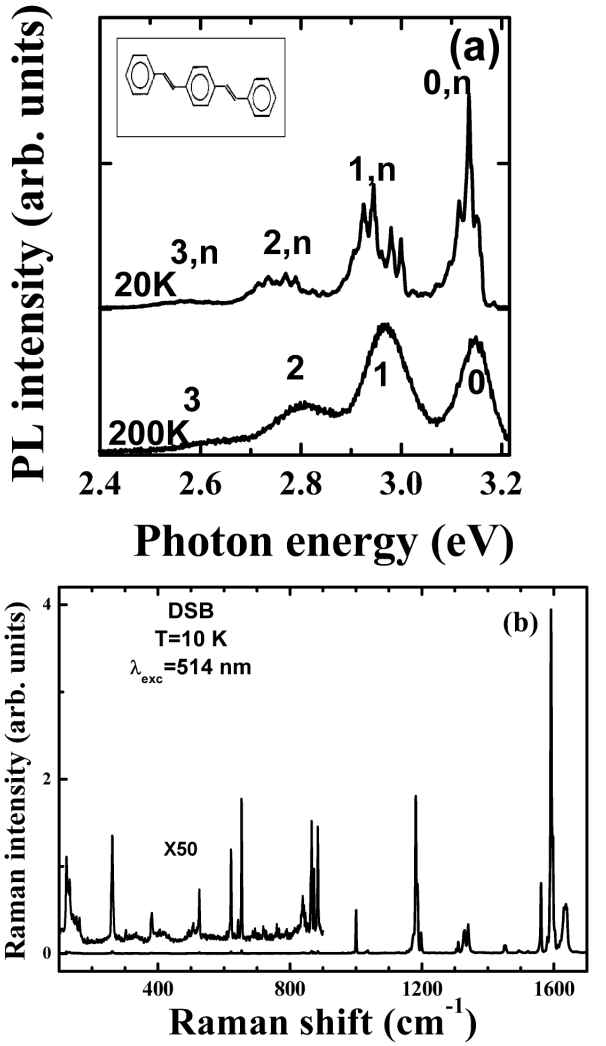

FIG. 2. (a) PL spectroscopy of DSB in solution at 20 and 200 K. The indices 0 and 1,2,3 in the 200 K spectrum denote the fundamental and vibronic replica transitions, respectively. The pairs of indices k, n (k=0,1,2,3) in the 20 K spectrum denote the complex modulated vibronic structure (see text). Inset: Chemical structure of DSB molecule. (b) High sensitivity preresonant Raman spectrum of DSB crystal at 10 K. The Raman frequencies and intensities are listed in Table 1.

In Fig. 2a we show the PL spectra of DSB in dilute frozen solution of tetradecane [11] at low and high temperatures. The measured PL spectrum at T=200 K has the typical vibronic progression shape as other π-conjugated systems, but notable changes occur with decreasing temperature. At T=200 K (Fig. 2a, bottom curve), there appears a dominant "high frequency" vibronic progression of ≈0.17 eV (≈1370 cm^{-1}), which, however does not match any of the Raman frequencies (Fig. 2b); it is not even in the close vicinity of the strongly coupled modes (Table I). The highest energy PL peak (marked "0") is interpreted as the fundamental optical transition ($1A_g \rightarrow 1B_u$), whereas the lower energy peaks (marked "1,2,3") are the vibronic side bands. At low temperatures, the high frequency progression is modulated by a different "low frequency" progression of ≈17-19 meV (Fig. 1a, T=20 K). We denote this modulated vibronic structure by k, n (k=0,1,2,3, n=0,1,2,...), where k (n) is the order of the high (low) frequency modulation.

Using the data of Table I we show in Fig. 3a the dipole auto-correlation function, f(t), generated for low and high damping. It is visually striking that the 11 mode system is dominated by only two apparent modes: a short period mode modulated by a long period mode. Moreover, the frequencies associated with these two modes do not coincide with any DSB normal mode. The data given in Table I is used also to generate the PL spectra shown in Fig. 3b. Here, the values of the electron temperature, T_e, HR factor S and damping Γ were adjusted to best fit the frozen solution experimental data at low and high lattice temperatures, T (Fig. 2a).

j	1	2	3	4	5	6
ν (cm^{-1})	131	261	640	873	1000	1181
I/I_{10}(%)	1.2	0.45	0.71	0.77	6.7	50
S	0.88	0.098	0.025	0.025	0.088	0.48
j	7	8	9	10	11	
ν (cm^{-1})	1330	1452	1561	1591	1635	
I/I_{10}(%)	19	2.7	13	100	42	
S	0.15	0.018	0.068	0.50	0.20	

Table I. The most intense Raman lines of DSB at T=10 K. ν, I and S are the frequency, relative intensity and HR factor, respectively, for each mode.

The higher damping spectrum that presumably occurs at T=200 K (Γ=42 ps^{-1}, Fig. 3b) shows a vibronic progression dominated by a single frequency of 173 meV (≈1400 cm^{-1}). These progression peaks are marked as "1,2,3". This is in excellent agreement with the experimental data at T=200 K (Fig. 2a, bottom curve). For this case we chose $T_e = T$, since the relevant modes are at high frequencies. At lower lattice temperatures we expect the damping to decrease. Consequently, the low frequency apparent mode is less suppressed, making the PL spectrum sensitive to the actual value of T_e. For low Γ values, there appears a low frequency modulation (≈17 meV) of the high frequency vibronic series, as seen in Fig. 3b (top curve). The combined progression peaks are denoted as (k,n), where k=0,1,2,3 denotes the high frequency apparent progression and n=0,1,2... denotes the low frequency modulation. The PL spectrum in Fig.

3b (top curve) was calculated using T_e=150 K; it shows two blue shifted peaks, in very good agreement with the experimental data at T=20 K (Fig. 2a, top curve). We thus conclude that due to the non-resonant PL excitation the electron temperature is much higher than the lattice temperature: $T_e > T$.

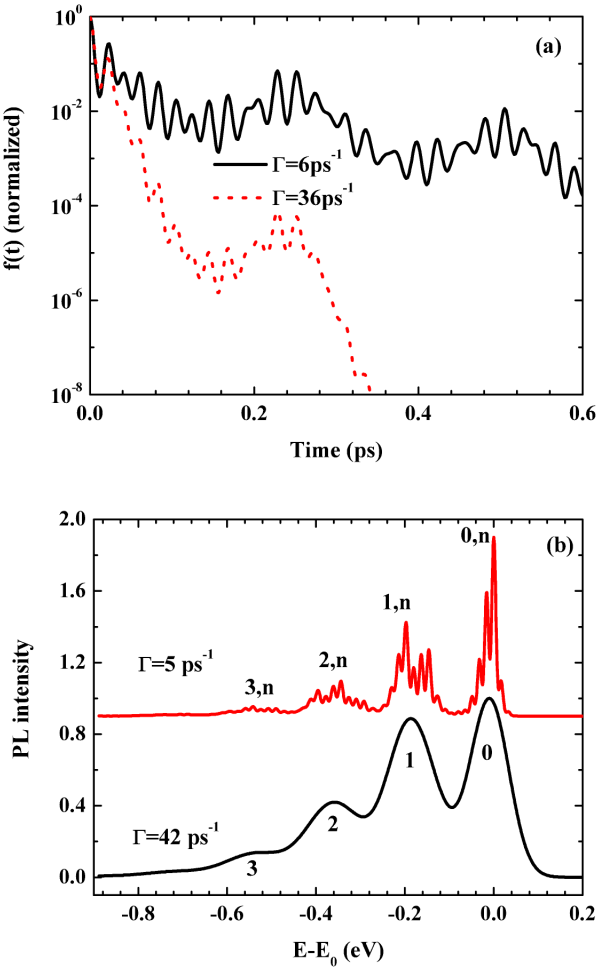

FIG. 3. Model calculations of PL spectra in DSB using the 11 mode system of Table I. (a) Normalized dipole auto-correlation function f(t) [Eqs. (2),(3)], for HR factor S(T=0)=2.5 and two values for Γ, as shown. Note the log scale. (b) PL spectra obtained by the Fourier transform of f(t) similar to that in (a), but for S(0)=1.7, T_e=150 (200) K for the upper (lower) curve and Γ as shown. The energy is measured relative to the fundamental transition.

In summary, we have shown that increased damping in multi-vibrational π-conjugated systems results in effective elimination of vibrational modes from the emission and absorption spectra and the eventual appearance of a nearly regularly spaced progression at an apparent frequency. We have presented a method by which measuring the full Raman spectrum, the emission spectrum of π-conjugated systems can be account for in detail. In particular, we interpret the blue shifted small peaks above the 0-0 transition, in the frozen DSB solution spectrum, as due to a "hot luminescence" process. In such a process, due to a high electron temperature, the first excited vibrational level is significantly populated.

Acknowledgments–Supported in part by DOE grant FG-04 ER46109 and by the Israel Science Foundation 735/04.

[1] H.S. Woo, S.C. Graham, D.A. Halliday, D.D.C. Bradley, R.H. Friend, Phys. Rev. B**46** (1992) 7379.
[2] E.J. Heller, R.L. Sundberg, D. Tannor, J. Phys. Chem. **86** (1982) 1822.
[3] S. Nakajima, Y. Toyozawa, R. Abe, "The Physics of Elementary Excitations", Springer Series in Solid State Sciences, Vol. 12, Springer Verlag, Berlin (1980).
[4] L. Tutt, D. Tannor, J. Schindler, E.J. Heller, J.I. Zink, J. Chem. Phys. **87** (1983) 3017.
[5] I. Orion, J.P. Buisson, S. Lefrant, Phys. Rev. B**57** (1998) 7050.
[6] F. Meinardi, M. Cerminara, S. Blumstengel, A. Sassella, A. Borghesi, R. Tubino, Phys. Rev. B**67** (2003) 184205.
[7] F.C. Spano, J. Chem. Phys. **114** (2001) 5376; **116** (2002) 5877; **118** (2003) 981; **120** (2004) 7643.
[8] G. Hadziioannou, in "Semiconducting Polymers: Chemistry, Physics, and Engineering", Eds. G. Hadziioannou, P. F. van Hutten, Wiley-VCH, New York (2000), Ch. 7.
[9] D. Oelkrug , H.-J. Egelhaaf, J. Gierschner, A. Tompert, Synth. Metals **76** (1996) 249.
[10] C.C. Wu, E. Ehrenfreund, J.J. Gutierrez, J.P. Ferraris, Z.V. Vardeny, Phys. Rev. B (Rapid Commun.), **71** (2005) 081201.
[11] J. Gierschner, H-G. Mack, L. Lüer, D. Oelkrug, J. Chem. Phys. **116** (2002) 8596.